SMALL-SCALE MAGNETIC FEATURES OBSERVED IN THE PHOTOSPHERE

Sara F. Martin
Big Bear Solar Observatory
Solar Astronomy 264-33
California Institute of Technology
Pasadena, CA 91214, U.S.A.

ABSTRACT. Small-scale solar features identifiable on the quiet sun in magnetograms of the line-of-sight component consist of network, intranetwork, ephemeral region magnetic fields, and the elementary bipoles of ephemeral active regions. Network fields are frequently observed to split into smaller fragments and equally often, small fragments are observed to merge or coalesce into larger clumps; this splitting and merging is generally confined to the borders and vertices of the convection cells known as supergranules. Intranetwork magnetic fields originate near the centers of the supergranule convection cells and appear to increase in magnetic flux as they flow in approximate radial patterns towards the boundaries of the cells.

Large ephemeral active regions which develop magnetic flux in excess of 5 X 10^{19}Mx often exhibit a secondary substructure of 'elementary bipoles' identical with the substructure that larger active regions exhibit during their first hours or day of development; the elementary bipoles often appear to berandomly oriented with respect to the axis of the initial bipole and these elementary poles often cancel with the initial poles or other elementary poles of opposite polarity.

Network, intranetwork and ephemeral region magnetic fields all encounter and interact with one another. Encounters of the same polarity result in the merger and adding of the magnetic flux from different features. Encounters of opposite polarity usually result in cancellation - the mutual disappearance of magnetic flux of opposite polarity at their common boundary. It is deduced that the mixed-polarity network originates primarily from the separated poles of ephemeral regions and secondarily from merged clusters of intranetwork fields.

1. Introduction

The small-scale magnetic features discussed in this paper are small relative to supergranules but are much larger than the smallest known magnetic elements in the the solar atmosphere. They consist of intranetwork magnetic fields, fragments of network, ephemeral active regions and the elementary bipoles of ephemeral active regions and active regions. Moving magnetic features around sunspots also are an important subject in the domain of small-scale magnetic features but their inclusion is beyond the scope of this paper. This paper will emphasize all other directly observable magnetic field structures in the range of 2-20 arc seconds in diameter. Structures of this scale are observable on an every-day basis. An advantage of studying structures in this range of scales is our current ability to observe their entire apparent lifetimes. A disadvantage is that the clarity of the observations is often affected by atmospheric turbulence.

Recent excellent reviews have thoroughly discussed the existence of much smaller magnetic

J. O. Stenflo (ed.), Solar Photosphere: Structure, Convection, and Magnetic Fields, 129–146.

structures than presented here. Both theory and techniques for determining the true dimensions of such small-scale magnetic elements have already been presented (Stenflo, 1989 and reviews cited therein). Thus, the features discussed here consist of clusters of smaller magnetic field elements and this knowledge is useful in the interpreting the observable evolution of features seen on time-series of magnetograms taken over intervals of several hours.

A full disk magnetogram from the USA National Solar Observtory site at Kitt Peak is shown in Figure 1. The date is 9 October 1988. On this magnetogram is a rectangle that corresponds to the field of view observed at the Big Bear Solar Observatory on the same day. The first objective is to examine the small-scale magnetic features within this limited field near the center of the solar disk and to describe how they change in a typical observing day in videomagnetograms from the Big Bear Solar Observatory.

2. Videomagnetogram Images and Data

A typical set of images taken at Big Bear Solar Observatory on 9 Oct 1988 in the 6103 A line of CaII is shown in Figure 2. Each set consists of a magnetogram at 512, 1024, 2048, and 4096 integrations. An integration is the smallest complete spatial and temporal unit of a videomagnetogram; it is pair of video images, one in each polarization, that have been electronically added to display the positive polarity as white and the negative polarity as black. This minimum magnetogram unit containing magnetic fields of both polarities can be displayed in 1/15 second, twice the standard video frame rate for a single frame. However, in order to see the magnetic fields, many such successive videomagnetogram units must be integated (added). Our local convention is to stop the integration of successive images in integral powers of 2. With the present system, it is necessary to take at least 2^{10} (1024) integrations to observe the weak magnetic fields on the quiet sun. However, the weak fields are more completely detected at 2048 and 4096 integrations.

On 9 Oct. 1988, a set of 4 such integrated images, as shown in Figure 2, was taken at intervals of 5 minutes throughout the 7.5 hour observing day. A five minute interval was chosen to minimize the effects of the solar 5 minute oscillations when one views the images of a selected number of integrations as a time-lapse movie. In the remaining illustrations in this paper, we use only the magnetograms with the highest number of integrations recorded on this day (4096).

The polarity in these videomagnetograms is determined by the color immediately outside of the contours. Positive polarity is white and negative polarity is black. Weaker fields are seen as shades of light gray for positive polarity and shades of dark gray for negative polarity. The areas within the contours represent magnetic fields that are stronger than can be displayed by the gray-scale range of our current image display system. For these images on 9 Oct. 1988, the lowest contour at 2048 integrations corresponds to fields of approximately 50 Gauss. The contours are introduced as a technique to show a more extended range of magnetic field strengths than can be readily distinguished in the gray-scale range alone. However, there also is a practical limit to the number of contours that can be displayed in small magnetic features on the sun at a given spatial resolution. If too many contours are introduced, the contours cannot be decoded for the purpose of calculating magnetic flux. For this reason, the magnetograms are taken in sets. The magnetograms with the higher numbers of integrations allow us to see and calculate the weak magnetic fields but the information in the strongest fields is lost. The magnetograms with lower integrations and

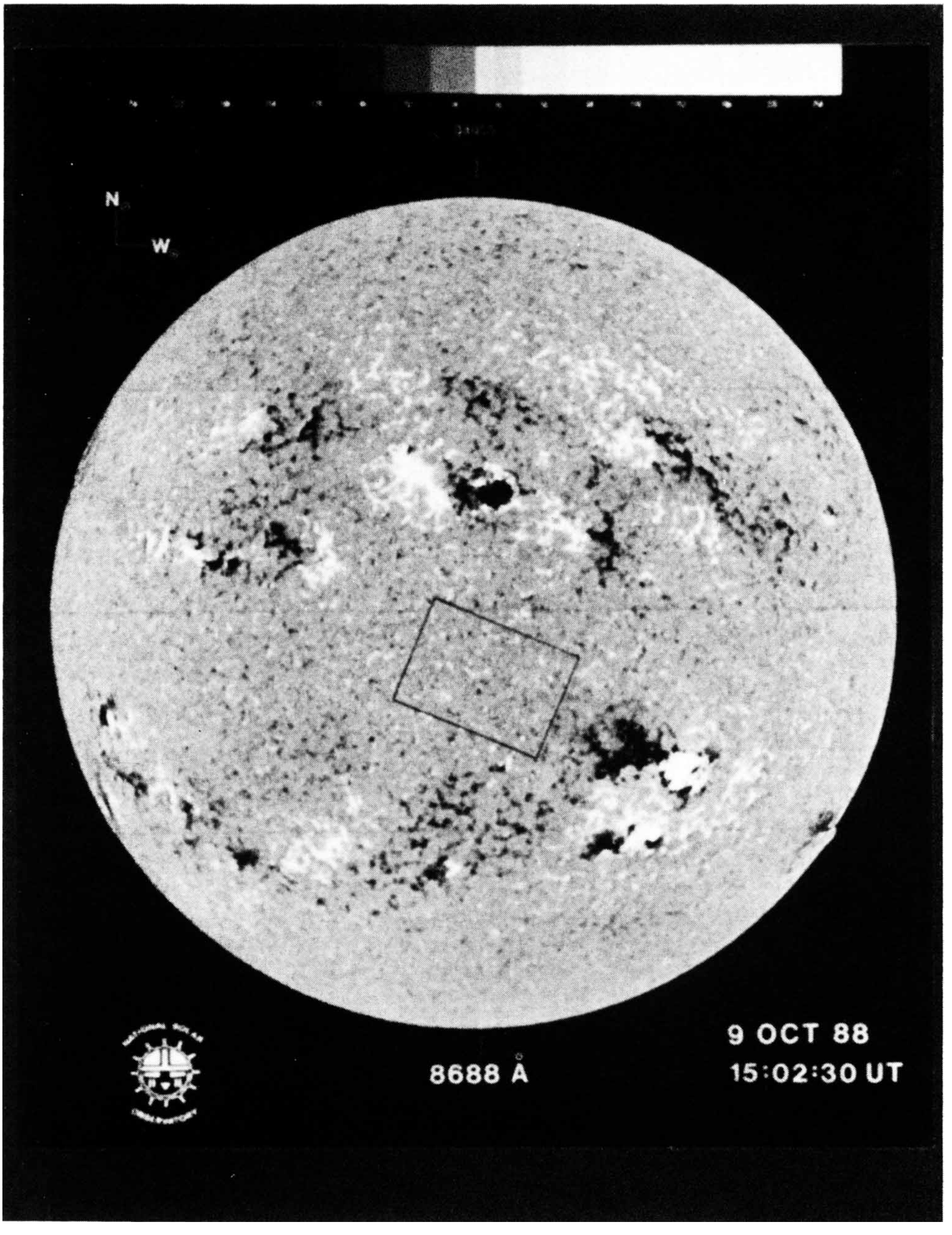

Figure 1. Magnetogram from USA National Solar Observatory taken on 9 Oct. 1988. The rectangle outlines the field of view containing weak-field, mixed-polarity network observed at Big Bear Solar Observatory on the same day.

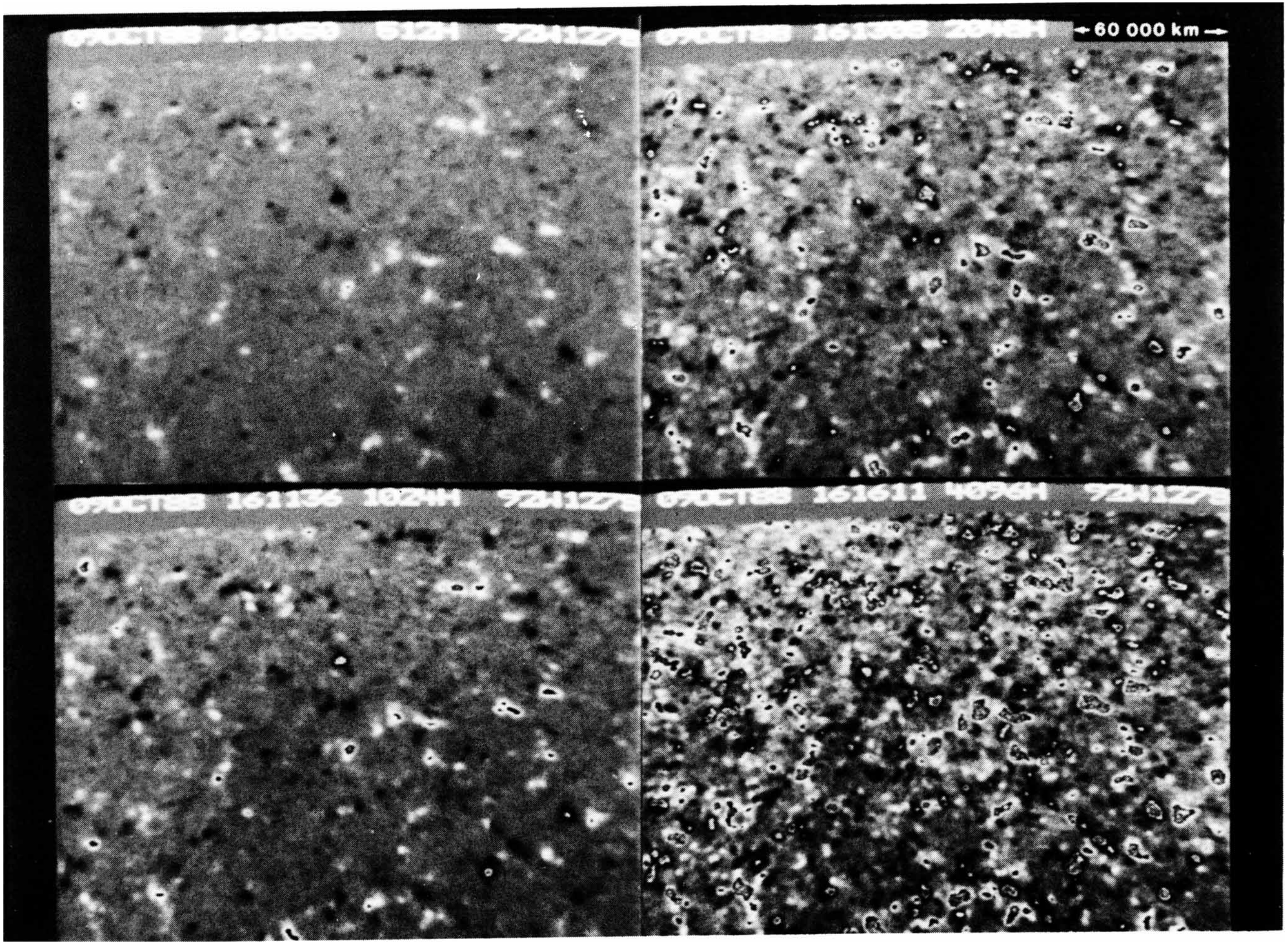

Figure 2. A set of consecutive magnetograms taken at the Big Bear Solar Observatory on 9 Oct. 1988 in order of increasing numbers of integrated video frame pairs: upperleft, 512; lower left, 1024; upper right, 2048; lower right, 4096. North is at the bottom and west at the left. The images must be rotated 180 degrees plus the position angle to be in the same orientation as the full-disk magnetogram in Figure 1.

https://doi.org/10.1017/S0074180900044077 Published online by Cambridge University Press

only a few contours are retained for combining images and for calculating the magnetic flux of the strong fields.

The magnetograms are recorded both in digital format on magnetic tape and also are displayed and photographed on a television monitor. Because the data is on magnetic tape, images can be selected and redisplayed in a variety of ways and at different stages of data processing. In our analyses we use both original and processed images. Decoding the contours and redisplaying the images in shades of gray makes the images easier to look at. Casual observers often would rather view the decoded images. However, during our analyses, we often prefer to use the original images with the contours because they better show a wider range of magnetic flux. For live presentations, different colors can be introduced in the contours of each polarity to make the visual interpretation easier.

3. The Identification of Magnetic Features

Reliable identifications of intranetwork, network and ephemeral region magnetic fields only can be done by studying time series of magnetograms. Even when one is very familiar with this type of data, it is not possible to correctly identify every feature on a single magnetogram. That is because the features evolve so rapidly that one often cannot distinguish between single poles of ephemeral regions and network fragments or between intranetwork patches and very small network fragments. These ambiguities are usually solved by taking time series of magnetograms. Then one can easily distinguish between ephemeral regions, network and intranetwork fields because each evolves and changes in characteristic ways.

If all features are studied together as a statistical sample, as done by Wang et al. (1989), no characteristic flux is identifiable. They found that the number of features always increases with decreasing feature flux above the threshhold of sensitivity. This means that network, ephemeral regions and intranetwork fields all have overlapping distributions of total magnetic flux per feature.

Figure 3 shows a magnetogram early in the observing day and another magnetogram late in the observing day. On the second magnetogram the network magnetic fields are enclosed in white polygons; new ephemeral regions are enclosed in solid-line black ovals; old ephemeral regions are enclosd in dashed black ovals. The remaining features, all notably small features, are intranetwork magnetic fields. The total flux in this magnetogram is 3.3×10^{21} Mx. Of this flux, 42% is in network magnetic fields (including the old ephemeral regions), 12% in new ephemeral regions and 46% in the intranetwork magnetic fields.

Because of the good image quality in these sets of observations, there is the opportunity to study the following:

1. the scale and dynamics of the intranetwork magnetic fields
2. characteristics of the mixed polarity network and its origin
3. the evolution and size distribution of ephemeral regions
4. the relationship of all of the above with respect to the evolution of supergranules

https://doi.org/10.1017/S0074180900044077 Published online by Cambridge University Press

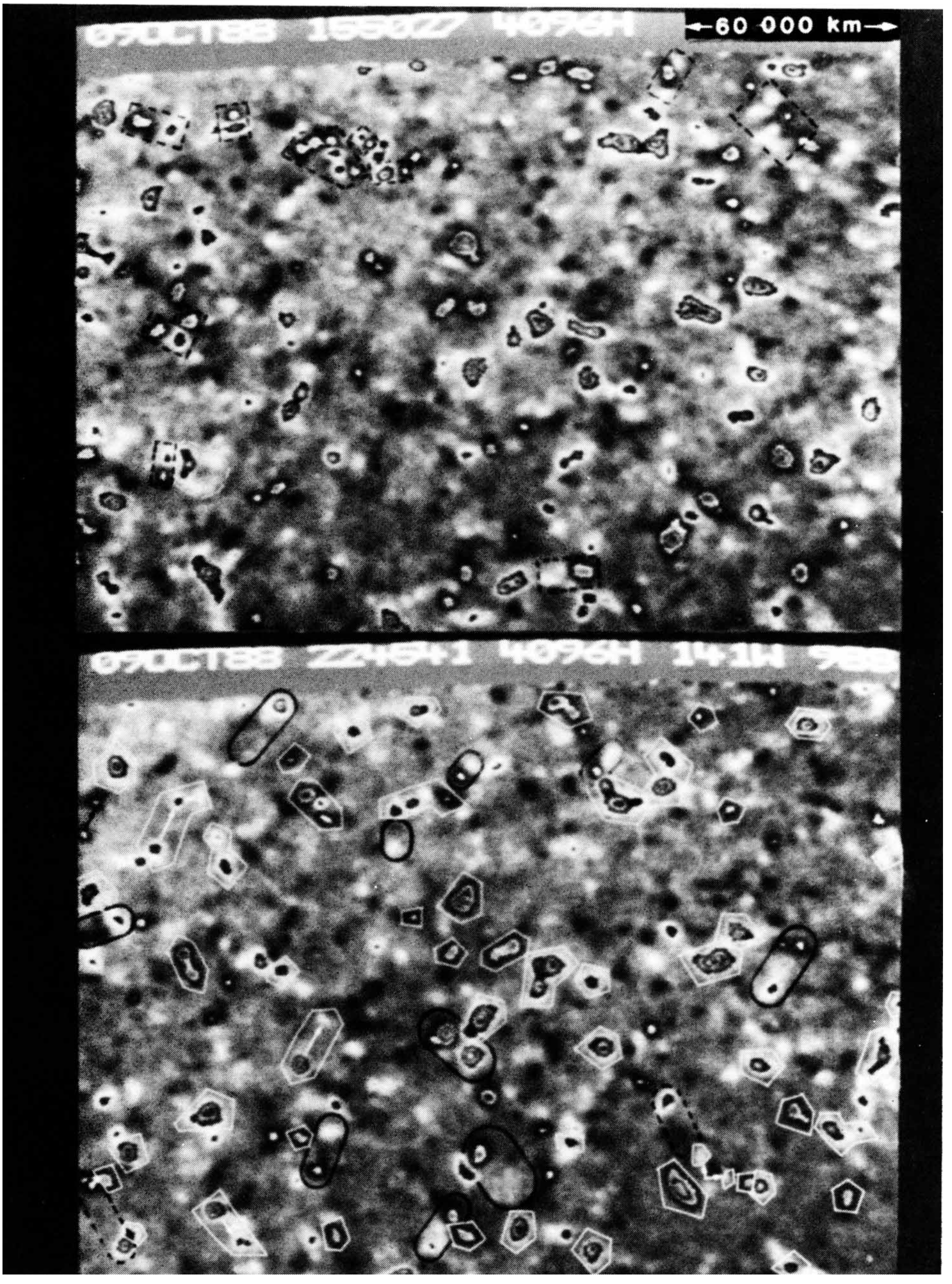

Figure 3. Magnetograms taken early and late on 9 Oct 1988. In the early magnetogram, prominent cancelling magnetic fields are enclosed in black, dashed rectangles or polygons. The dashed white polygon encloses intranetwork patches which coaslesce around the larger area of positive polarity network. In the later magnetogram new ephemeral regions observed from birth are enclosed in solid-line, black ovals and older ephemeral regions in dashed ovals. Network fragments that were observed throughout the day are enclosed in solid-line white polygons. The remaining small patches of field in between the ephemeral regions and network are the intranetwork magnetic fields.

https://doi.org/10.1017/S0074180900044077 Published online by Cambridge University Press

4. Network Magnetic Fields

Network magnetic fields are identified within the polygons in the lower half of Figure 3. These network features are all of the ones that could be traced as a persistent features since the beginning of the observing day. Persistent does not imply a lack of change - only that part of a network cluster is traceable for many hours. As seen in Figure 3, the majority of the network features have changed substantially from the beginning until the end of the day. The types of changes that can be seen in the network in the time-series of magnetograms are:

(1) splitting into smaller fragments,
(2) gain in flux due to merging with neighboring network, intranetwork, or ephemeral region fields of the same polarity,
(3) decrease in flux from encountering and polarity, or
(4) combinations of (1)-(3).

Examples of the merging and splitting of network fragments are illustrated by Martin (1988). The network includes most of the largest areas of magnetic flux in the field-of-view but also includes many small fragments which are comparable to the scale of the small intranetwork fields. The smallest areas of network magnetic flux shown here are ones that originated from the fragmentation (splitting) of larger network elements. Such small network elements do not usually survive as independent entities for more than a few hours without merging with other network or intranetwork patches or cancelling with any opposite polarity fields that are encountered. The arrows show the direction and distance of travel for some of the fragmented areas of network.

5. Ephemeral Active Regions

An ephemeral active region is a small bipole in which its opposite polarities:
(1) appear adjacent to each other at nearly the same time
(2) increase in magnetic flux and
(3) move in opposite directions as the region increases in magnetic flux, at least until one of the poles encounters external opposite-polarity field comparable to its magnitude at the time of encounter.

Every ephemeral regions in Figure 3 developed at least one saturation contour at sometime during the observing day. Our threshhold for identification is therefore a peak flux of at least 50 Gauss in at least one pole. However, no ephemeral regions were observed on this day that did not fit this criteria. The solid ovals include the 10 of the 11 ephemeral regions whose birth was observed during the 7.5 hour observing day. The one not shown was on the extreme right edge of the field of view and observations of it were incomplete. The two dashed ovals are ephemeral regions not observed from birth but are identifiable from their characteristic pattern of growth and motion. Old ephemeral regions (ones that have reached or passed their peak magnetic flux) are usually indistinguishable from the mixed polarity network in single images. The two old ephemeral regions in Figure 3 were identified while viewing the data as a time-lapse movie; the one in the lower right quadrant of Figure 3, at the time shown, lost its negative pole from cancelling with opposite polarity network. Both poles of the one in the lower left corner have merged with network of the same polarity and similar magnitude. Both of the old ephemeral regions were included in the 42% of the fields designated as network magnetic fields.

It is seen also in Figure 3 that many (at least 6) of the 11 new ephemeral regions have also encountered and either merged or cancelled with network fields. Thus it is apparent that ephemeral regions are one of the possible sources of the mixed polarity network. The ephemeral regions contribute to both cancellation and resupplying of the mixed polarity network. This topic is further discussed in Section 7.

In addition to interacting with the network magnetic fields, ephemeral regions also interact with intranetwork magnetic fields. The fine structure of ephemeral regions is also at least as small as the observable intranetwork fields. Figure 4 illustrates the development of an ephemeral region and typical interactions with intranetwork fields. It is the same ephemeral region with several contours seen in the middle of the second image in Figure 3. This ephemeral region, like many this size and larger, is first seen as more than just a single pole of each polarity. At 1714 UT, the positive pole is initially seen as three small, separate dots. These merge by 1748 to form the primary positive pole. The negative pole of the ephemeral region grows at a site where a small, negative polarity (black) intranetwork patch already existed at 1628. The intranetwork patch and the negative ephemeral region pole are indistinguishable from each other at 1702. An adjacent positive-polarity (white) intranetwork patch also partially cancels with the negative ephemeral region pole but then migrates toward the positive pole and merges with it. An new elementary bipole is seen at 1834 within the oval between the original poles of the ephemeral region. The negative (black) pole is visible as early as 1748, also between the primary poles of the ephemeral region.

To the right of the positive pole, another positive (white) intranetwork magnetic patch concentrates and develops a single contour. By 1903 it merges with the positive pole of the ephemeral region to form a single magnetic feature.

We tend to think of ephemeral regions just as growing bipoles because that is an essential part of our definition of an ephemeral region. However, this example illustrates how parts of an ephemeral region can merge with adjacent features of the same polarity and cancel with adjacent magnetic features of opposite polarity. Cancellation is defined as the disappearance of both polarities at a common boundary in line-of-sight magnetograms (Martin, Livi and Wang, 1985; Livi, Wang and Martin, 1985). Cancellation is not a rare, isolated phenomenon but rather a process that is typical when opposite polarity features encounter one another. The interpretation of cancellation is briefly discussed in Section 9.

The cancellation and merging of ephemeral regions with adjacent network and intranetwork fields is the primary reason that the magnetic flux of ephemeral regions is rarely balanced between the two poles (Livi, Wang and Martin, 1985). The distribution of flux in the poles of ephemeral regions and between their individual poles is shown in Figure 5 at the time of the second image in Figure 3. The magnetic flux in the ephemeral regions at 2257 UT (excluding one which is partly out of the field of view) is 2.0 X 10 Mx. The individual ephemeral regions range in total flux from 4.8 to 47.7 X 10 Mx. There is no known lower limit to the size of an ephemeral region. The upper limit is arbitrary because there are no distinctive physical properties of individual ephemeral active regions that separate them from small active regions (Harvey, Harvey and Martin 1975). The statistical distributions of ephemeral regions by latitude, magnitude, and inclination of their magnetic axes have all been shown to blend smoothly into the statistical distributions of active region (Harvey, Harvey and Martin 1975; Martin and Harvey 1979, Harvey 1988) with the exception of one study by Tang, Howard and Adkins (1984). This single discrepancy is resolved by the study of Harvey (1989) which shows the spectrum of active regions, small active regions and ephemeral

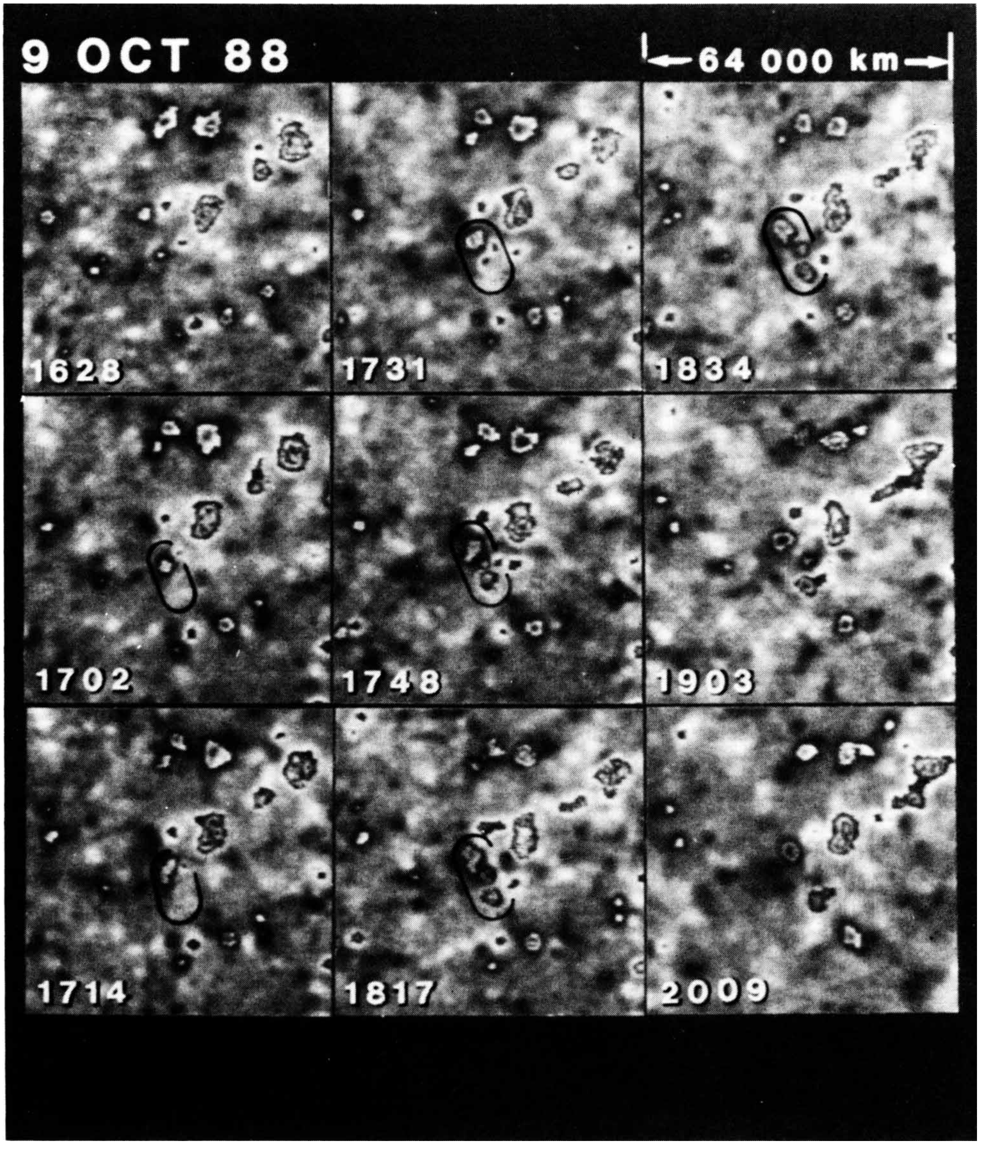

Figure 4. The new magnetic flux of an ephemeral region is first recognizable at 1702. The new negative pole coincides with a pre-existing negative polarity intranetwork patch. At 1714 the new positive pole is initially seen as 3 separate positive patches which then merge together by 1748. A secondary elementary bipole is visible between the initial poles at 1834. The negative elementary pole became visible at 1748 before the appearance of the positive pole.

https://doi.org/10.1017/S0074180900044077 Published online by Cambridge University Press

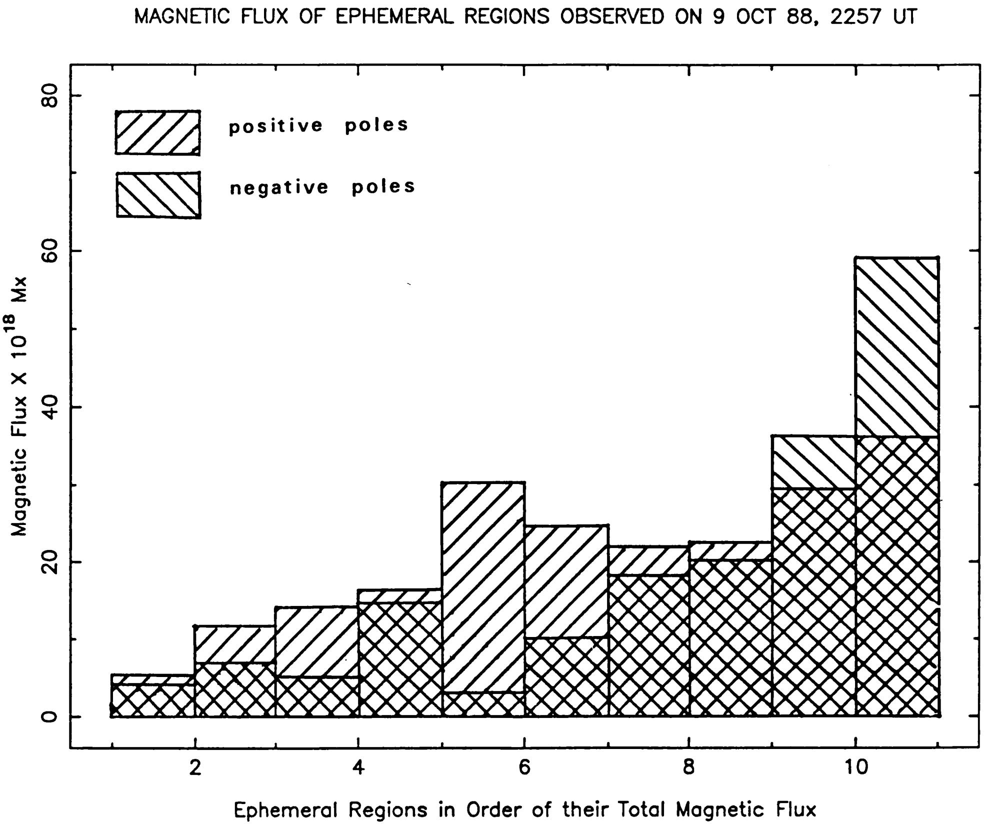

Figure 5. The magnetic flux in the poles of the ephemeral regions ranged from 3 to 36 X 10^{18} Mx at 2257 UT on 9 Oct. 1988. The imbalance between the poles of the ephemeral regions was found to be due to the coalescence and cancellation of the ephemeral region magnetic flux with adjacent network and intranetwork magnetic features.

https://doi.org/10.1017/S0074180900044077 Published online by Cambridge University Press

active regions to be continuous rather than discontinuous. Our arbitrary convention is to call new bipolar regions ephemeral regions if they develop insufficient concentrated magnetic flux to form sunspots. Sunspot pores form whenever concentrations of flux exceed approximately 10^{20}Mx (Harvey and Martin, 1973; Zwaan 1978, 1985; Chou and Wang, 1987).

6. Intranetwork Magnetic Fields

Intranetwork patches rarely survive more than a few hours. They originate in the centers of supergranules and typically flow at a rate of approximately 0.35 km s^{-1} (Zirin, 1987) until they encounter either network, ephemeral regions or other intranetwork fields from adjacent supergranule cells. If the encountered fields are the same polarity, the intranetwork fields merge with them. If the encountered fields are of opposite polarity, the intranetwork fields cancel with the encountered fields.

As the intranetwork fields flow from the centers to the boundaries of the supergranule cells, they increase in magnetic flux and area. The increase in flux might be due to the merging of adjacent fields or to a change in the direction of the magnetic field such that a larger fraction of the line-of-sight component is detected. The merging of adjacent intranetwork fields is observable both before the intranetwork patches reach the network boundaries as well as at the boundaries. A cluster of merging intranetwork patches are enclosed in the dashed white polygon In the lower left quadrant of the upper frame in Figure 3. In the lower frame in Figure 3, it is seen that the merger of these intranetwork patches has resulted in about a 50% increase in the flux of the network fragment around which the intranetwork fields coalesce.

In magnetograms composed of successively lower integrations (2048, 1024 and 512), the intranetwork field patches appear to originate within increasingly larger annuli with respect to the centers of the cells. This effect is due to both the lower magnetic sensitivity in magnetograms with lesser numbers of integrations and the apparent increase in flux as the intranetwork fields flow approximately radially toward the cell boundaries.

Figure 6 shows the migration of intranetwork patches toward a isolated concentration of negative polarity network magnetic field. The network fragment is isolated and relatively stationary with only small variations in flux throughout the day. It is located at the vertices of several supergranule cells. It is continuously interacting with approaching intranetwork fields which converge towards it from the adjacent supergranule cells. The positve intranetwork fields cancel with (diminish) the network fragment while a comparable number of negative polarity intranetwork fields merge with (add to) the network fragment. Since each cancellation and merger occurs slowly and involves small quantities of flux (on the order of 10^{18} Maxwells per hour), the total flux of the network fragment changes very little during the course of the day.

7. The Elementary Bipoles of Ephemeral Active Regions and Active Regions

The appearance of new elementary bipoles are characteristic small-scale features seen in ephemeral active regions whose total flux is of the order 10^{19} Mx and in larger, new active regions. Only the ephemeral region with the greatest magnetic flux, observed on 9 Oct. 1988 (Figure 4), developed a secondary elementary pair of poles after the development of the initial pair of poles. However, most similar high integration, high quality observations of

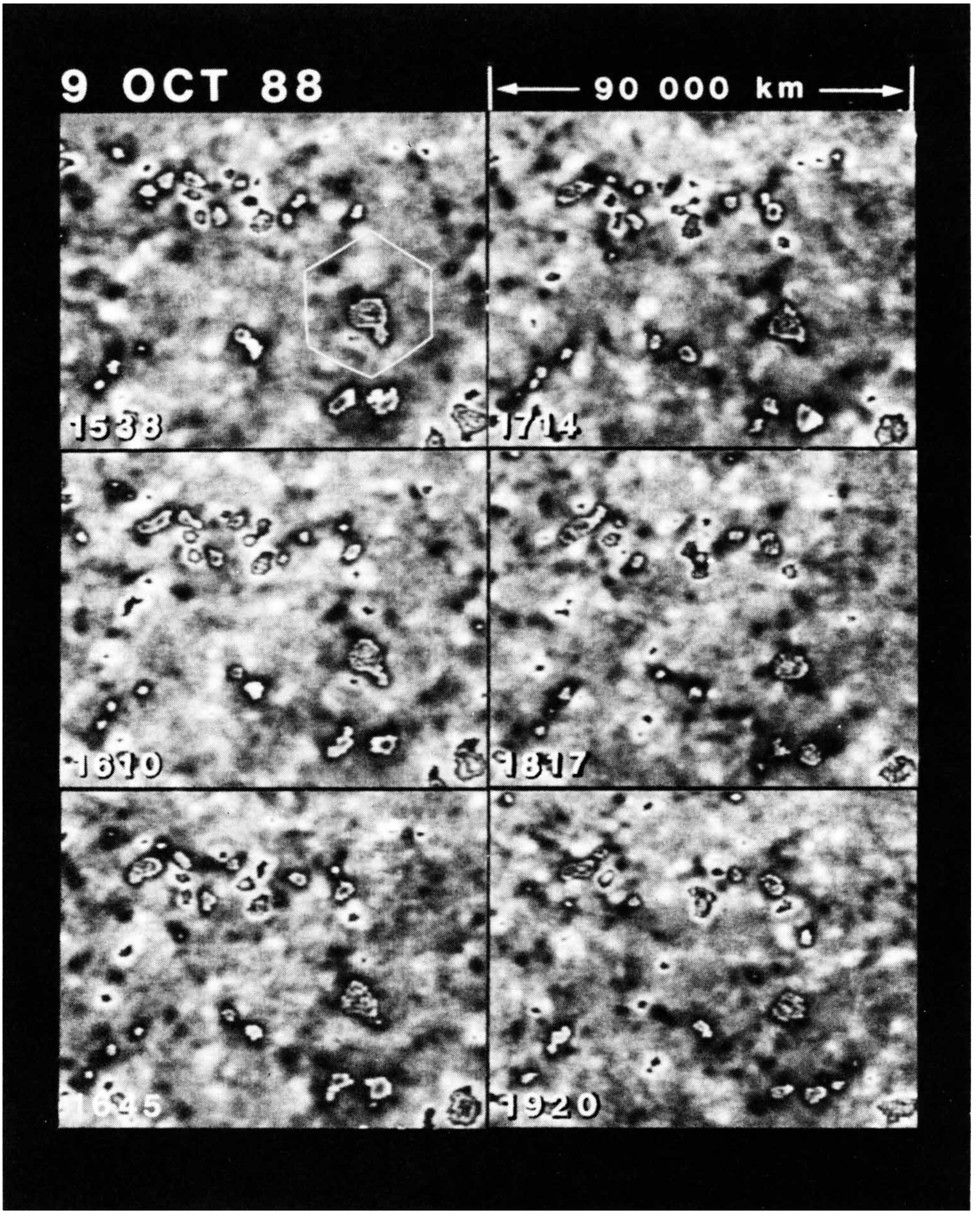

Figure 6. Within the white polygon, intranetwork magnetic field patches are seen to flow toward the area of network. The network fragment is at the vertices of several adjoining supergranule cells. In the upper left, a complex cluster of network magnetic fields of both polarities converge and cancel at another vertices between adjoining supergranule cells. The flux slowly reduces in this cluster throughout the observing day due to the cancellation of opposite polarity fields.

new ephemeral active regions and new active regions show the development of these secondary bipoles. Frazier (1972) has shown that the development and separation of these elementary bipoles, which he called 'magnetic knots', typically occurs under arch filament systems in Hα observations. Frazier (1972) and Vrabec (1974) found examples of the magnetic knots streaming into sunspots with speeds of approximately 0.3 km s when sufficient flux had accumulated for sunspots to form.

In the videomagnetogram observations collected at the Big Bear Solar Observatory, it can be seen that the elementary bipoles of both ephemeral regions and active regions often do not develop in the same orientation as the original pair or pairs of poles. If they develop with a reversed orientation from the original pair, they seem to be destined to cancel with previously emerged magnetic flux because the elementary poles separate from each other in the same way that first ephemeral region poles or active region poles move apart as their flux increases. Examples of secondary elementary bipoles are shown in the ephemeral active region and active regions illustrated respectively in Figures 7 and 8.

In Figure 7 the ephemeral region is first seen at 1732. The poles increase in magnetic flux and separate. Near the site of emergence of the original bipole, a secondary elementary bipole appears but its orientation is reversed from the original pair. The negative pole of the secondary bipole begins to cancel with the original positive pole and then becomes surrounded by the positive polarity fragments. After the complete cancellation of the negative elementary pole, the positive fragments coalesce into single unresolved pole. This positive pole then begins to cancel with the adjacent negative polarity network fragment. The predictable end of this sequence is that the negative pole of the ephemeral regions will remain and will become indistinguishable from any other network fragment.

The number of elementary bipoles increases for active regions of increasing ultimate area and magnetic flux. Examples of two small new active regions are shown in Figure 8. The region on the left has a whole cluster of elementary poles that are evolving and interacting. At the beginning of this sequence it is not clear which elementary poles originated at pairs. They seem to be randomly oriented. Some of the elementary poles of opposite polarity cancel and some of similar polarity merge. Overall the number of the mergers of similar polarity outnumber the elementary poles that cancel and the region grows.

The bipolar active region on the right has only one negative elementary pole at the beginning of this series; it is cancelling and disappears completely by 2003. Overall this bipolar active region has reached its maximum development. However that does not mean the flux is static. The negative pole is cancelling throughout this series with positive polarity magnetic flux of the other active region. At the same time, the positive polarity fragments are slowly increasing in magnetic flux at least until 2215. In addition, at the end of the observing day one more new elementary bipole appears above the primary negative pole in the last frame at 2314.

Small scale magnetic fragments are also seen during the decay of active regions. Numerous examples of small-scale cancelling fragments of magnetic flux are described and illustrated by Martin, Livi and Wang (1985) and Martin et al. (1989). They have shown that cancellation can account for the disappearance of either large quantities or all of the flux within some active regions.

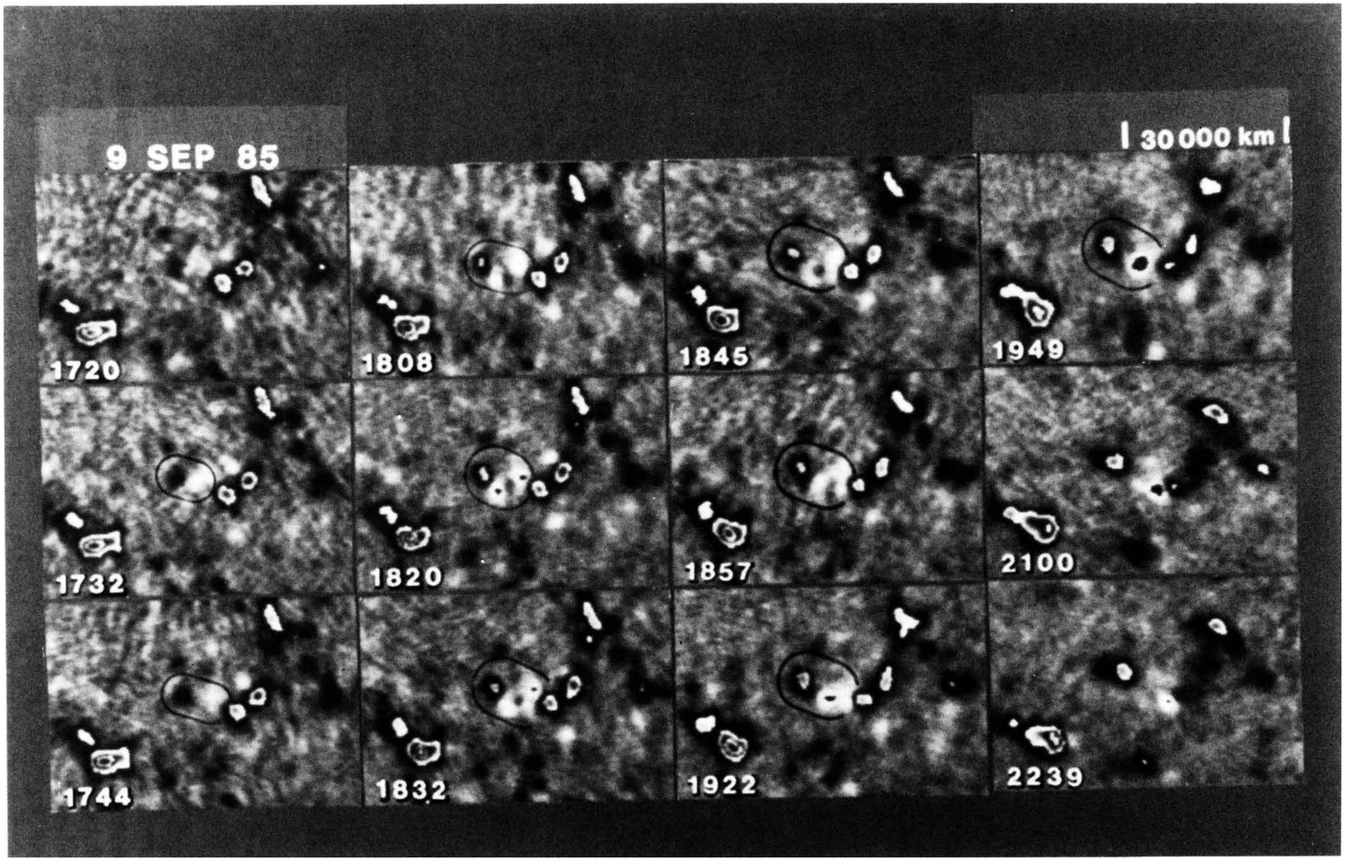

Figure 7. The initial poles of an ephemeral region are first seen at 1732. An elementary bipole appears between the initial poles at 1808. Note that the new elementary bipole is reversed in orientation from the poles of original bipole. The reversed negative pole cancels with the surrounding positive polarity patches until it completery disappears at 1922. Then the positive poles of the original and secondary bipoles coalesce into a single patch (1949) and thereafter cancel with the adjacent negative-polarity network. The surviving negative pole of the ephemeral region becomes part of the network.

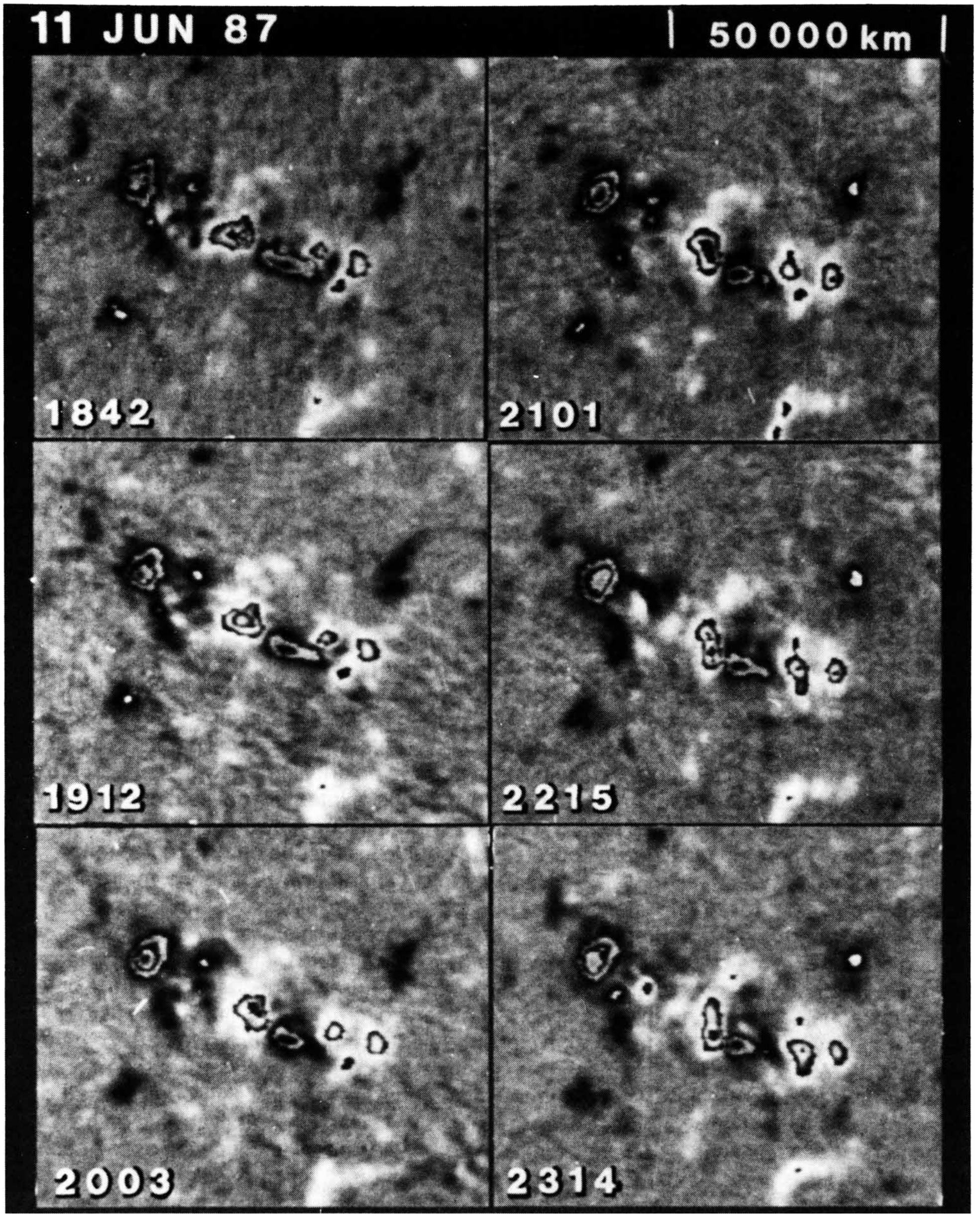

Figure 8. Two small active regions appear side-by-side. The one on the left is still growing as seen by the appearance of new elementary bipoles. The one on the right is cancelling at nearly the same rate that it is growing. Cancellation takes place where opposite polarity fields move together: withing the growing region, within the decaying region, and at the boundary between the two regions.

https://doi.org/10.1017/S0074180900044077 Published online by Cambridge University Press

8. Origin of the Mixed-Polarity Network

Near the end of the day as shown in the lower half of Figure 3, 12% of the magnetic flux in the whole field of view was in new ephemeral regions, 42% in network fields and old active regions, and the balance of 46% of the flux was from the background intranetwork magnetic fields. The relative percentages of magnetic flux distributed among the different features depends on observational factors. In general the detectability of the intranetwork fields depends strongly on the number of integrations in the magnetograms. It also depends strongly on seeing and image stability which vary throughout the day and from day to day. Thus, the above percentages give us only a general idea of the proportion of magnetic flux among the differing classes of magnetic features. However, it is important to note that the intranetwork fields comprise about half of the magnetic flux in a quiet sun field of view where mostly mixed-polarity network is present. The amount of unipolar and mixed-polarity network varies greatly over the solar surface at any given time as well as over the solar cycle (Giovanelli, 1982). The number of ephemeral regions likewise varies with latitude and time during the solar cycle (Harvey, Harvey, and Martin, 1975; Martin and Harvey, 1979).

The mixed polarity network does not constitute new magnetic flux. It must therefore originate from either or both ephemeral regions or the intranetwork magnetic fields. The amount of ephemeral region flux and intranetwork flux that could contribute to the mixed polarity network depends not only on the ratio of the features in a given field-of-view but also on their mean survival time. Survival time in turn depends on the amount of time from initial appearance until encounter with adjacent features and on the average rate of cancellation with opposite polarity fields.

From this set of observations it can be seen that the intranetwork fields make a contribution to the mixed polarity network. The coalescence (and cancellation) of intranetwork fields which originate in adjacent cells are directly observable. Such coalesced intranetwork fields of the same polarity can become network elements by themselves or merge with other network fragments. An example is the cluster of positive polarity intranetwork fields at the extreme right side of the lower frame in Figure 3. Groups of intranetwork field of the same polarity are sometimes observed to add substantially to existing network elements. One of the network elements in the field was observed to double in size due only to coalescence with intranetwork fields. This example is the positive polarity intranetwork patches enclosed in a dashed polygon in the lower left corner of the upper frame in Figure 3.
The intranetwork clusters marked in Figure 3 are the largest such clusters that were observed to contribute to the network during this observing day. I estimate that the contribution to the mixed-polarity network from temporary clusterings of intranetwork patches is 10% or less. Since the ephemeral regions are the only other observed form of new flux in this field of view, I conclude that 90% or more of the mixed-polarity network must originate from the separated poles of ephemeral regions. This is consistent with the observed duration of the ephemeral regions. All 11 of the 11 ephemeral regions had traceable flux or were still growing at the end of the 7.5 hour observing interval. Hence, the survival time of the ephemeral region flux must be several times the observing interval. Since the observations cover slightly less than one-third of the observing day, about 3 times this amount of flux appears in the form of ephemeral regions each day in this field. If the ephemeral region flux has an average survival time of only 3.5 times the observing interval, then most or all of the mixed-polarity network could be accounted for by just the dispersed ephemeral region flux.

9. Interpreting the Observations of Cancelling Magnetic Flux

As seen in magnetograms of the line-of-sight component, the majority of magnetic fields on the both the quiet sun and in active regions disappear by cancellation of opposite polarity fields that encounter one another[1m. The characteristics of cancelling magnetic fields have been described in Martin (1984), Livi, Wang and Martin (1985), Martin, Livi, and Wang (1985), Wang et al. (1988) and Martin et al. (1989).

The disappearance of magnetic flux by cancellation can be interpreted as submergence or magnetic field reconnection (Zwaan 1985, 1987). Because ephemeral regions, as illustrated here, originate as bipoles but cancel with external features, I favor the interpretation as magnetic reconnection. Because the cancellations of ephemeral region poles with network and intranetwork fields have the same properties as cancellations between all other solar fields, (network fields, intranetwork fields and active region fields), one mechanism is sufficient to explain all cases of observed cancelling fields of opposite polarity.

A spectrum of regimes of magnetic reconnection have been discovered by Priest and Forbes (1986). I suggest that the type of reconnection associated with 'cancellation' is at the opposite end of the spectrum of reconnection regimes from the type of reconnection commonly associated with solar flares. Flare reconnection is rapid, leads abrupt energy release, and has no signature in present-day, photospheric magnetograms. In contrast, the type of reconnection resulting in 'cancellation' is slow, is associated with very weak, long-enduring enhancements in hydrogen-alpha filtergrams, and is a commonly observed phenomena in photopheric magnetograms of the line-of-sight component of magnetic fields. Because cancellation is associated with increasing magnetic field gradients (Wang et al., 1988), I suggest that cancellation is most easily associated with 'magnetic pile-up reconnection' among the magnetic reconnection regimes described by Priest and Forbes (1986). More work in observing or deducing the 3 dimensional magnetic structures at cancellation sites is needed to obtain a better understanding of this phenomenon.

10. Summary

The quiet sun is composed is composed of three classes of magnetic features: ephemeral active regions, network and intranetwork magnetic fields. It is deduced that the mixed-polarity network originates primarily from surviving separated poles of ephemeral active regions but some network elements are also observed to form from the coalescence of similar polarity patches of intranetwork magnetic flux that merge at the boundaries of supergranule cells.

During their growth phase, both ephemeral active regions and active regions are characterized by the appearance of secondary elementary poles which successively evolve between the initial poles of a new region. Although many elementary bipoles develop with approximately the same orientation as the original poles, some also develop with reversed or random orientations with respect to the original poles of a new region; elementary poles with reversed orientations from the original poles usually cancel with the original poles or other elementary bipoles.

Ephemeral active regions and active regions also cancel with adjacent intranetwork, network or active region magnetic fields. These external cancellations are the primary reason why the magnetic flux of the poles of ephemeral active regions are rarely balanced.

https://doi.org/10.1017/S0074180900044077 Published online by Cambridge University Press

The observations of cancelling magnetic features are interpreted by the author as representing a type of magnetic reconnection described as 'magnetic pile-up reconnection' in the spectrum of reconnection regimes found and described by Priest and Forbes (1986).

Acknowledgements

This study was supported by the Air Force Office of Scientific Research under contract AFOSR-87-0023.

References

Chou, D. and Wang, H.: 1987, *Solar Phys.* **110**, 81.
Frazier, E.N.: 1972, *Solar Phys.* **26**, 130.
Giovanelli, R.G.: 1982, *Solar Phys.* **77**, 27.
Harvey, K.L.: 1989, in preparation.
Harvey, K.L. and Martin, S.F.: 1973, *Solar Phys.* **32**, 389.
Harvey, K.L., Harvey, J.W. and Martin, S.F.: 1975, *Solar Physics* **40**, 87.
Livi, S.H.B., Wang, J. and Martin, S.F.: 1985, *Australian J. Phys.* **38**, 855.
Martin, S.F. 1988, *Solar Phys.* **117**, 243.
Martin, S.F. and Harvey, K.L.: 1979, *Solar Phys.* **64**, 93.
Martin, S.F. Livi, S.H.B. and Wang, J.: 1985, *Australian J. Phys.* **38**, 929.
Priest, E.R. and Forbes, T.G.: 1986, *J. Geophys. Res.* **91**, 5579.
Stenflo, J.O.: 1989, Astron. Astrophys. Review 1, 3.
Tang, F., Howard, R.F. and Adkins, J. M.: 1984, *Solar Phys.* **91**, 76.
Vrabec, D.: 1974, in R.G. Athay (ed.), '*Chromospheric Fine Structure',* IAU Symp. **56**, 201.
Wang, J., Shi, Z., Liu, J. Han, Feng and Liu, G.: 1989, presented at IAU Symp. 138, Kiev, 14-19 May 1989.
Wang, J., Shi, Z., Martin, S.F. and Livi, S.H.B.: 1988, *Vistas in Astronomy,* **31**, 79.
Zirin, H.: 1987, *Solar Phys.* **110**, 101.
Zwaan, C.: 1978, *Solar Phys.* **60**, 213.
Zwaan, C.: 1985, *Solar Phys.* **100**, 397.
Zwaan, C.: 1985, in R. Muller, *Lecture Notes in Physics,* Vol. **233**, Springer-Verlag, Berlin, p.263.
Zwaan, C.: 1987, *Ann. Rev. Astron. Astrophys.* **25,** 83.